The Adsorption of Polymerized Rodlike Micelles at the Solid−Liquid Interface

Simon Biggs,[†] Steven R. Kline,[‡] and Lynn M. Walker*,[§]

School of Process, Environmental and Materials Engineering, University of Leeds, Leeds LS2 9JT, United Kingdom, NIST Center for Neutron Research, 100 Bureau Drive, Stop 8562, Gaithersburg, Maryland 20899-8562, and Department of Chemical Engineering, Center for Complex Fluids Engineering, Carnegie Mellon University, Pittsburgh, Pennsylvania 15213

Solutions of rodlike polymeric micellar aggregates, formed from the polymerization of cetyltrimethyl-ammonium 4-vinylbenzoate (CTVB), adsorb at the solid−liquid interface. The poly-CTVB aggregates are imaged in situ using soft contact atomic force microscopy. The aggregates form self-organized two-dimensional films that show a high degree of order on nanometer to micrometer length scales. Unlike their simple surfactant analogues, the adsorbed layer structures are permanently adsorbed and the structure is resilient to washing with pure solvent. In the case of poly-CTVB, the adsorbed aggregates appear to be rigid cylindrical structures of between 30 and 60 nm in length. At the interface, the center to center spacing of the aligned aggregates is 8 ± 1 nm. Images of a second series of polymerized aggregates formed by the copolymerization of CTVB with sodium vinyltosylate revealed a change in the aggregate structure to a set of linked spherical aggregates. These polymerized aggregates also spontaneously form a permanent adsorbed layer at the solid−liquid interface.

Introduction

The interfacial self-assembly of complex structures from molecular building blocks offers many opportunities in the design and manufacture of new materials.[1] A requirement of the self-assembly process is that it results in macroscopic structures, with long-range order, that have some degree of local molecular order on nanometer length scales. An example would be a close-packed array of surfactant micelles. These new materials are of interest as a result of the novel properties that may arise when a characteristic length scale of the structure becomes comparable to that of a given physical phenomenon, for example, electron-transfer processes.[2] Furthermore, the resultant surfaces are heterogeneous with regions that can have different chemical or physical properties. Such surfaces have many potential uses including as template structures for the formation of more complex nanostructures or nanodevices.[3]

The production of organized molecular surface coatings has a long history. The most successful technology to date for the production of molecular films is based upon Langmuir−Blodgett (LB) deposition techniques. Using such approaches, researchers have successfully manufactured complex films consisting of many repeat layers having a high degree of spatial organization.[4] Unfortunately, the production of LB films requires very specialized equipment, it is limited to macroscopic flat substrates, and it requires molecules capable of forming an ordered film at a solvent−air or solvent−solvent interface. These limitations are severe when issues of real world applications and device manufacture are considered. Attempts to resolve these problems, while still being able to produce organized molecular films, have centered on functionalized molecules that can react chemically with surface groups to produce a covalently anchored layer. The production of so-called "self-assembled monolayers" (SAMs) has been demonstrated with many molecules on a variety of substrates although the most popular combination has been thiolated molecules on gold surfaces.[5] In a recent review, Decher[6] notes that, despite their popularity for surface modification, such films have a number of inherent problems. Foremost among these are a limited film stability over time, steric restrictions that can limit packing efficiency (and hence film integrity), and a difficulty in producing multilayers.

Recently, it has been shown conclusively that surfactants form micelle-like structures when adsorbed at the solid−liquid interface.[7] In particular, the use of atomic force microscopy (AFM) has revealed a wide range of possible adsorbed layer structures that rival the rich variety seen in bulk. For example, structures such as spheres, rods, and tubules have been observed as well as the more standard monolayers and bilayers.[8] These structures are obviously appealing as surface templates because they form spontaneously and the individual aggregates have a controlled local physicochemical heterogeneity. Furthermore, there is considerable structural order between the aggregates over relatively large surface areas. An example of the possibilities of synthesizing secondary organized structures that are templated by these surfactant layers has recently been reported.[9]

[†] University of Leeds.
[‡] NIST Center for Neutron Research.
[§] Carnegie Mellon University.
(1) Rao, C. N. R.; Cheetham, A. K. *J. Mater. Chem.* **2001**, *11*, 2887−2894.
(2) Collins, P. G.; Zettl, A.; Bando, H.; Thess, A.; Smalley, R. E. *Science* **1997**, *278*, 100−103.
(3) Jirage, K. B.; Hulteen, J. C.; Martin, C. R. *Science* **1997**, *278*, 655−658.
(4) Adamson, A. W.; Gast, A. P. *Physical Chemistry of Surfaces*; Wiley-Interscience: New York, 1997.

(5) Whitesides, G. M.; Laibinis, P. E. *Langmuir* **1990**, *6*, 87−96.
(6) Decher, G. *Science* **1997**, *277*, 1232−1237.
(7) Manne, S.; Cleveland, J. P.; Gaub, H. E.; Stucky, G. D.; Hansma, P. K. *Langmuir* **1994**, *10*, 4409−4413.
(8) Warr, G. G. *Curr. Opin. Colloid Interface Sci.* **2000**, *5*, 88−94.
(9) Aksay, I. A.; Trau, M.; Manne, S.; Honma, I.; Yao, N.; Zhou, L.; Fenter, P.; Eisenberger, P. M.; Gruner, S. M. *Science* **1996**, *273*, 892−898.

The interest in organic surfactant materials arises largely from the enormous chemical diversity available and hence the large potential for subtle variations in structures and properties. Despite this, a significant limitation on the use of these surfactant-based surface structures arises from the requirement for a significant bulk concentration of the same surfactant to be present at all times. Thus, subsequent processing steps at the surface may be significantly affected or even prevented. It is also apparent that removal of the bulk surfactant solution and drying of the surface will result in a complete loss of structural integrity. Finally, it should also be noted here that such self-assembled molecular systems are highly susceptible to variations in atmospheric conditions such as temperature, pH, solvent type, or dehydration.[10]

The desire to generate surface structures that are more robust to subsequent processing steps has led to the investigation of block copolymers and their micellar aggregates as the fundamental building blocks for surface structures.[11−14] A major advantage of polymeric surfactants is that their adsorption to a substrate is effectively irreversible.[15] Thus, after adsorption the coated surfaces can be removed from solution or the solution can be altered without necessarily having a detrimental effect on the layer. Currently, the majority of reports relating to the formation of such films are based on deposition by spin coating that produces dried monolayer films that are subsequently rehydrated. For example, Spatz and co-workers have recently reported the deposition of poly-(styrene)-*block*-poly(2-vinylpyridine) [PS-*b*-P2VP] and poly(styrene)-*block*-poly(ethylene oxide) [PS-*b*-PEO] copolymer micelles onto transmission electron microscopy surfaces by spin coating from a good solvent (toluene) for the PS blocks.[13,14] The spacing between the micelle cores was observed to depend on the molecular weight of the coronal blocks which is attributed to steric repulsions during film drying. In situ formation of ordered films at the solid−liquid interface has only recently been reported for copolymer micelles in an aqueous environment.[11,16] Initial data suggest that good control over micelle packing (radial distribution and spacing) can be obtained. While block copolymer micelles may yet offer an interesting route to nano-organized structures, the interaggregate spacing (center−center) is typically of the order of 10−100 nm. Thus, new materials, which depend on one or more characteristic length scales being less than 10 nm, may prove elusive from this route.

An alternative method for the production of functional organized structures arises from the microphase separation observed when block copolymers are solvent cast onto solid substrates.[17,18] Judicious choice of the copolymer blocks molecular weights and chemistries allows for the formation of a range of structures such as lamellae,

cylinders, or spheres. However, the opportunities for subsequent rehydration and processing are frequently severely limited for these systems.

Our approach is based upon the use of a polymerized micellar aggregate. One of us has recently reported the successful production of polymerized rodlike micelles using ionic surfactants in which the counterion is a polymerizable material.[19,20] The reported system was based on the surfactant cetyltrimethylammonium 4-vinylbenzoate (CTVB). This surfactant spontaneously forms entangled wormlike aggregates at concentrations well above its critical micelle concentration (cmc). Upon polymerization, detailed analysis of the structure indicates that it is consistent with an uncharged cylinder. In general, polymerization was seen to result in a reduction in the length of the cylinders but the retention of the cross-sectional area and structure. The novelty of these polymerized aggregates is that the micellar structure is apparently "locked-in" and we observe relative insensitivity to environmental changes. The aggregate structure is not influenced by moderate changes in the ionic strength or temperature of the solutions. Furthermore, the aggregates can be freeze-dried and resuspended in water without loss of the structure.[21] Furthermore, since the aggregates are polymeric in nature, we expect their adsorption to be permanent, allowing washing and subsequent processing of any surface adsorbed layers formed.[15]

Experimental Section

Samples and Substrates. All water used here was purified by reverse osmosis and subsequent passage through a MilliQ Plus (Millipore) system. Circular, amorphous silica cover slips (ESCO Products, S1-UV P/N R412000) that are 12 mm in diameter were used as the silica substrate. These were cleaned and soaked in basic solution and then soaked in copious amounts of distilled water prior to use. Muscovite mica surfaces were freshly cleaved in a laminar flow cabinet immediately prior to use. Atomic force microscopy images and force data were used to confirm that these surfaces were clean and free of contamination. Details of the monomeric surfactants, their polymeric analogues, and the salt used in this investigation are summarized in Table 1. The CTVB monomer and its polymeric analogues were synthesized in-house. Details of the synthesis and purification for these molecules are given elsewhere.[19]

Atomic Force Microscopy. We used a Nanoscope III AFM (Digital Instruments) to image adsorbed surfactant and polymerized surfactant films using the "soft-contact" mode described previously.[7,22] In this mode, the adsorbed film is imaged in situ using the repulsive double layer forces that exist between the imaging tip and the surface to maintain the tip at a constant and finite separation distance. The probes used here were standard silicon nitride cantilevers that have an imaging tip with a nominal radius of 50 nm and a spring constant of 0.1 N/m. The cantilevers were irradiated in UV plasma for 45 min immediately prior to use. The AFM liquid cell, imaging probe, and clean surface were assembled for use within a laminar flow unit immediately prior to an experiment. In a typical experiment, water was first injected into the liquid cell. Images of the surface and force curves were then used to confirm the surfaces were clean. At this point, the solution of interest was injected into the liquid cell. All changes of solvent or solution were performed using a large excess of the new solution. Images of the surface adsorbed layers were then collected after a minimum equilibration time of approximately 30 min.

All images are presented here as deflection images. These images were collected with proportional and integral gains of 1 and at scan rates of 1−2 Hz. No filtering of the images was

(10) Hunter, R. J. *Introduction to Modern Colloid Science*; Oxford University Press: Oxford, 1993.

(11) Talingting, M. R.; Ma, Y. H.; Simmons, C.; Webber, S. E. *Langmuir* **2000**, *16*, 862−865.

(12) Spatz, J. P.; Sheiko, S.; Moller, M. *Macromolecules* **1996**, *29*, 3220−3226.

(13) Spatz, J. P.; Mossmer, S.; Hartmann, C.; Moller, M.; Herzog, T.; Krieger, M.; Boyen, H. G.; Ziemann, P.; Kabius, B. *Langmuir* **2000**, *16*, 407−415.

(14) Regenbrecht, M.; Akari, S.; Forster, S.; Mohwald, H. *J. Phys. Chem. B* **1999**, *103*, 6669−6675.

(15) Fleer, G. J.; Stuart, M. A. C.; Scheutjens, J. M. H. M.; Cosgrove, T.; Vincent, B. *Polymers at Interfaces*; Gordon and Breach: London, 1993.

(16) Webber, G. B.; Wanless, E. J.; Armes, S. P.; Baines, F. L.; Biggs, S. *Langmuir* **2001**, *17*, 5551−5561.

(17) Muthukumar, M.; Ober, C. K.; Thomas, E. L. *Science* **1997**, *277*, 1225−1232.

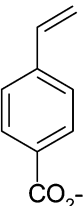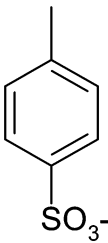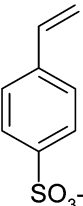(18) Lopes, W. A.; Jaeger, H. M. *Nature* **2001**, *414*, 735−738.

(19) Kline, S. R. *Langmuir* **1999**, *15*, 2726−2732.

(20) Kline, S. *J. Appl. Crystallogr.* **2000**, *33*, 618−622.

(21) Gerber, M. J.; Walker, L. M. Unpublished results.

(22) Fleming, B. D.; Wanless, E. J. *Microsc. Microanal.* **2000**, *6*, 104−112.

Table 1. Compositions of Materials Used in This Study[a]

Compounds used (mole fraction)	Counterion structure	Polymerized	Conc. (gm/L)	Designation
CTVB	vinyl benzoate (CO_2^-)	No	0.14	CTVB
CTVB		Yes	0.8	poly-CTVB
CTVB + NaT (2:1)	tosylate (SO_3^-)	No	0.13	CTVB:NaT
CTVB + NaVT (2:1)	vinyl tosylate (SO_3^-)	Yes	1.0	poly-CTVB:NaVT

[a] Polymerization was performed at 60 °C in 1 wt % total surfactant concentration and 5 mol % initiator relative to the monomer concentration (see ref 19). CTVB denotes cetyltrimethylammonium vinylbenzoate, NaT denotes sodium tosylate, and NaVT denotes sodium vinyltosylate.

performed other than that inherent in the feedback loop of the instrument. Distances in all three dimensions were independently calibrated using a standard etched grid.

Results and Discussion

The main focus of this investigation is a structural analysis, using AFM, of adsorbed layers formed by polymerized surfactant systems. Two polymeric micellar systems have been investigated here, poly-CTVB and poly-CTVB:NaVT. The poly-CTVB system was chosen since its bulk behavior and structure have been characterized.[19] The poly-CTVB:NaVT system demonstrates the structural diversity possible as subtle changes in counterion composition lead to aggregates with different structure and charge. In each case, for comparison, a nonpolymerized analogue was also examined.

In the bulk, CTVB forms rodlike micelles at concentrations a few times its cmc, the cmc of CTVB is reported to be 0.16 mM (0.07 gm/L).[19] The micellar cross section has been measured using SANS and found to be 2.1 nm. Figure 1 shows a 500 × 500 nm image of CTVB adsorbed on mica. The image indicates clearly the presence of aggregates at this interface. The aggregates have one long axis and one short; the long axes are apparently aligned over distances

on the order of 50–100 nm. Along one of the aggregates there is some evidence of small deviations about the average direction. A Fourier transform of the data is shown as an inset to Figure 1, showing two bright arcs. Analysis of the radial position of the arcs in the transform indicates that the peak-to-peak spacing between the cylinders is 9.5 ± 0.5 nm. This distance corresponds to the sum of the aggregate diameter and the intermicellar separation at the interface. The azimuthal position of the two bright arcs indicates a preferred orientation for the aggregates as is seen in the image. This spacing is reported for all solutions and surfaces studied in Table 2.

Force versus separation data, collected for the interaction of the imaging tip with the surface, have previously been used to estimate the thickness of an adsorbed layer of surfactant. Data of this type, collected on the same sample presented in Figure 1, are shown in Figure 2. This data set is representative of many taken on this surface, all show the same quantitative behavior. Starting at large separation distances, movement of the two surfaces toward each other initially results in no deflection of the cantilever. In this region the force of interaction is effectively zero. As the separation distance is reduced further, a repulsive force is recorded. This "long-range" force component is
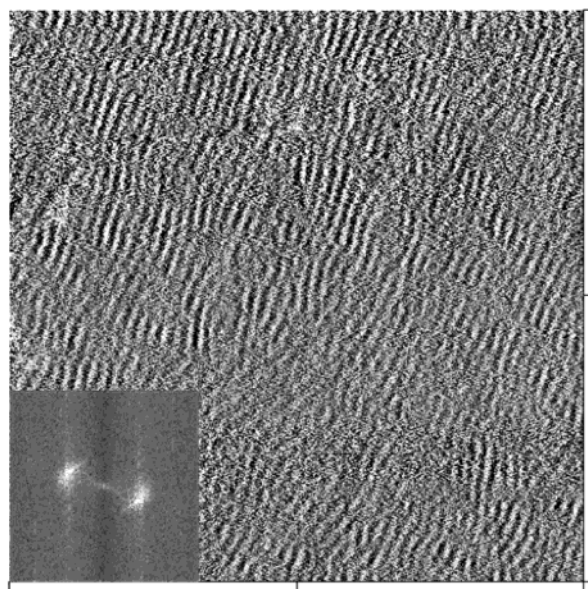
Figure 1. 500-nm AFM deflection image of adsorbed CTVB at the mica−solution interface. The images were obtained in situ, at a surfactant concentration of 0.14 g/L (>2 × cmc) using a soft-contact imaging protocol. The presence of long cylinders at the interface is clearly visible. The inset to this figure shows the Fourier transform of the data. The presence of two arcs indicates that the axes of the cylinders only deviate a small amount over the image size.

Table 2. Characteristic Dimensions of Adsorbed Layers on Two Different Surfaces[a]

components	surface	mean aggregate spacing (nm)	"jump-in" distance (nm)
CTVB	mica	9.5 ± 0.5	2.1 ± 0.5
CTVB	silica	7.4 ± 0.3	4.2 ± 0.5
poly-CTVB	mica	8.3 ± 0.3	4.2 ± 0.5
poly-CTVB	silica	7.2 ± 0.3	4.2 ± 0.5
CTVB:NaT	mica	8.3 ± 0.3	3.7 ± 0.2
CTVB:NaT	silica	6.9 ± 0.2	4.3 ± 0.2
poly-CTVB:NaVT	mica	8.4 ± 0.2	
poly-CTVB:NaVT	silica	8.1 ± 0.2	

[a] Average aggregate spacing is determined from FFT of images while "jump-in" is extracted from representative force curves.
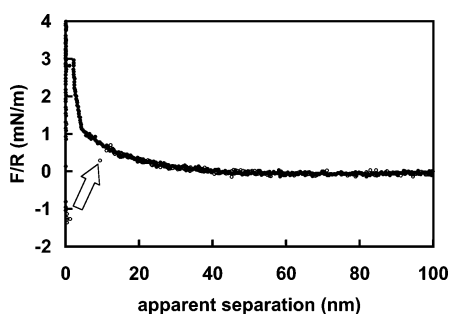

Figure 2. Force as a function of separation distance for the interaction between a silicon AFM tip and a mica surface in 0.14 g/L CTVB. Data are shown for both the approach (filled) of the tip to the surface and its retraction (open). The arrow indicates the adhesive pull-off and jump outward of the tip from the surface.

attributed to the repulsive double layer interactions between the adsorbed ionic surfactant films. At a separation of 5.2 ± 0.5 nm there is a transition in the form of the interaction and further reduction in the separation results in a steeply repulsive interaction before an instability at 2.1 ± 0.5 nm. The steeply repulsive region is thought to result from the tip pushing down on the

adsorbed surfactant layer. At some point, the force exerted is large enough to push through this layer and a jump-in to the surface results. This is qualitatively, but not quantitatively, similar to previously reported data for CTA^+ surfactants at the mica−solution interface.[7,23,24] Again, this "jump-in" distance is reported for all solutions and surfaces in Table 2. Reversal of the direction of surface movement results in an initial adhesive interaction between the surfaces. Eventually, the restoring force of the tip is sufficient to overcome the adhesion between the surfaces and a jump-out of the tip from the surface is seen. Again these data are consistent with previous reports.

There are no previous reports of the adsorption of CTVB at the solid−liquid interface. By contrast, the adsorption of CTAB (cetyltrimethylammonium bromide) at the mica−solution interface has received considerable attention in the literature.[7,23,24] In the absence of added electrolyte, and above the bulk solution cmc, CTAB initially forms an adsorbed film that has a similar appearance to that seen here, i.e., meandering cylinders. However, over several hours this structure develops into a featureless bilayer.[24] Addition of more than 10 mM of a simple electrolyte such as KBr is sufficient to prevent this transition, and the cylindrical structures are observed to persist. In contrast, for CTVB no electrolyte was required to stabilize the cylindrical structures at the mica−solution interface. Our measurements indicate that these structures are stable for more than 24 h. In the case of CTAB, the addition of salt is known to facilitate a transformation in the bulk from spheres to cylinders. According to the concepts of the packing-parameter model,[25] this transition results from a decrease in the repulsive interaction between surfactant headgroups which allows a lower curvature structure to form.[26] On mica, analogous charge compensation effects are thought to occur.[23,24] In the absence of added electrolyte, interaction with charged surface sites significantly lowers the repulsive interactions and allows the ultimate formation of a zero curvature structure (bilayer). Addition of electrolyte results in competition between the headgroups of the surfactant and the added cations for the surface charge sites. This leads to a decreased adsorption of the headgroups in the layer immediately adjacent to the surface and hence increased curvature of the adsorbed aggregates.

The persistence of the cylindrical CTVB aggregate structures at the mica−solution interface, in the absence of added electrolyte, reflects the bulk solution behavior of this molecule.[19] CTVB is known to form elongated worm-like micelles in bulk solution (above the cmc) without the need for added electrolyte. The difference in bulk behavior, when compared to CTAB, is mirrored by the difference in the surface behaviors.[25] As noted above, the formation of cylindrical or wormlike micelles is related to the headgroup repulsions.[26] These are effected by electrolytic screening effects and by the degree of counterion condensation at the surface of the micelle.[23,27,28] The degree of counterion binding is determined by a number of factors including charge density of the headgroup and the counterion as

(23) Lamont, R. E.; Ducker, W. A. *J. Am. Chem. Soc.* **1998**, *120*, 7602−7607.

(24) Ducker, W. A.; Wanless, E. J. *Langmuir* **1999**, *15*, 160−168.

(25) Vinson, P. K.; Bellare, J. R.; Davis, H. T.; Miller, W. G.; Scriven, L. E. *J. Colloid Interface Sci.* **1991**, *142*, 74−91.

(26) Israelachvili, J. N.; Mitchell, D. J.; Ninham, B. W. *J. Chem. Soc., Faraday Trans. 2* **1976**, *72*, 1525−1568.

(27) Patrick, H. N.; Warr, G. G.; Manne, S.; Aksay, I. A. *Langmuir* **1999**, *15*, 1685−1692.

(28) Subramanian, V.; Ducker, W. A. *Langmuir* **2000**, *16*, 4447−4454.

well as the degree of hydration of the ions. Counterions that have a significant organic character are also known to affect the degree of condensation since they have a strong tendency to penetrate into the micelle core.[29] In the case of CTVB, the counterion is large and has a significant organic character. It is expected that there will be significant condensation in this case. This is supported by the image of the adsorbed layer, which shows cylindrical aggregates. It is also interesting that this layer does not evolve with time into a featureless bilayer, as seen in the case of CTAB.[24] This is despite the extremely high density of surface charge groups on mica and must be related to the extremely small dissociation of the CTVB molecules from the aggregate. The slow evolution of structure in the case of CTAB from cylinders to a bilayer was attributed to the slow exchange of K^+ and Br^- ions out of the initially formed cylindrical surface structures.[24] It was argued that this is caused by increased electrostatic effects within the surfactant film which hinders ionic release. Only after ions have exchanged out of the layer can the CTA^+ ions bind to the surface-charged sites and produce a flat bilayer film. If we consider that Br^- ion release from the cylindrical micelles is relatively facile when compared to the vinylbenzoate ions used here, it is hardly surprising that cylindrical aggregate structures persist over time for CTVB.

It should be noted here that it is impossible to distinguish from images between a layer of hemispherical "half" cylinders on an underlying monolayer of surfactant and a layer of full cylinders. The "jump-in" distance of 2.1 ± 0.5 nm recorded here is small when compared to previous data for CTA^+ surfactants. The presence of charge on the aggregates, initially proposed from SANS data, is confirmed from the force data. Interaction of the charged CTA^+ ions with the mica interface may therefore be expected, even if it is insufficient to promote a bilayer structure. Previously, it has been suggested that the jump-in point occurs when sufficient force is exerted to allow a lateral displacement of the adsorbed aggregates. For spherical structures this corresponds to their diameters. In this case, the smaller than expected jump-in corresponds to approximately one extended CTA^+ molecule and may result from the displacement of a hemispherical layer initially followed by penetration through a heads-down monolayer of the CTA^+ molecules. This picture is consistent with the force data in which the initial lateral displacement of a hemispherical layer, which is sufficiently weak not to register on the force data, is followed by a penetration of a heads-down monolayer of the CTA^+ molecules, which is seen in the force data. Alternatively, the smaller than expected jump-in distance may result from a flattening of the cylindrical aggregates at the interface. This point will be discussed further below, after presentation of data for the silica surface.

Previous reports have indicated that the surface can significantly influence the adsorbed layer structure.[23,30] For example, CTAB solutions in the absence of added electrolyte adsorb as spherical "micelle-like" aggregates at the surface of silica and as a featureless bilayer on mica. The differences are caused by the higher surface density of charge groups on mica leading to a more efficient charge neutralization of the CTA^+ ions and hence a lower curvature structure. Once again, the CTAB system can be induced to form an adsorbed layer of cylinders on silica by the addition of electrolyte. The effect of a change from
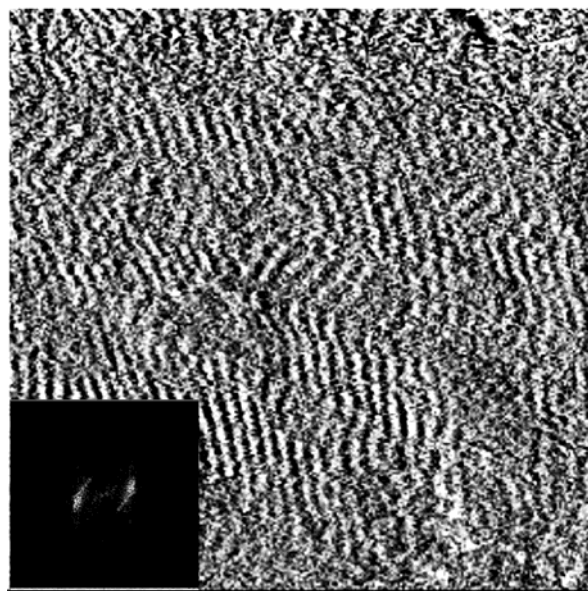
(29) Bijma, K.; Blandamer, M. J.; Engberts, J. *Langmuir* **1998**, *14*, 79−83.

(30) Liu, J. F.; Ducker, W. A. *J. Phys. Chem. B* **1999**, *103*, 8558−8567.

Figure 3. 400-nm AFM deflection image of adsorbed CTVB at the silica−solution interface. The images were obtained in situ, at a surfactant concentration of 0.14 g/L (>2 × cmc). The presence of long cylinders at the interface is clearly visible. The inset to this figure shows the Fourier transform of the data.
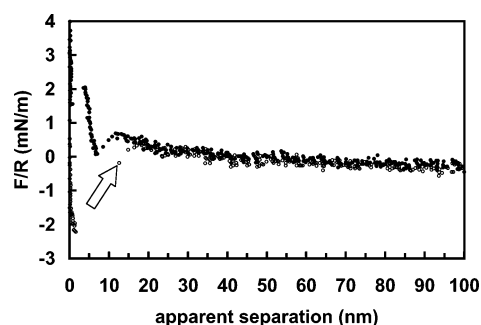

Figure 4. Force as a function of separation distance for the interaction between a silicon AFM tip and a silica surface in 0.14 g/L CTVB. Data are shown for both the approach (filled) of the tip to the surface and its retraction (open). The arrow indicates the adhesive pull-off and jump outward of the tip from the surface.

mica to silica was also investigated here. An image of the adsorbed equilibrium layer at the surface of silica is shown in Figure 3. Corresponding force−distance data are shown in Figure 4. The image of the adsorbed film does not exhibit excellent resolution. This is most likely due to difficulties in attaining a stable imaging force in the soft-contact mode. However, the partial image collected here clearly shows a series of parallel meandering stripes reminiscent of the structure seen on the mica surface. A two-dimensional Fourier transform of these data is also consistent with the same structure having been formed. The peak-to-peak interaggregate spacing determined from these data is 7.4 ± 0.3 nm. The strong association between the CTA^+ ion and its counterion has prevented any significant surface influence, and the bulk structure persists at the interface. Adsorbed cylindrical micelles, in the absence of added electrolyte, have previously been observed for CTAB with added NaS (sodium salicylate).[27] Salicylate ions are also known to bind strongly to the micelle surface and facilitate the formation of wormlike aggregates in bulk solution. Subramainen and Ducker[28] have systematically investigated the effects of counterion type, against the CTA^+ ion, for adsorbed layer structures on silica. The degree of counterion condensation was seen to increase in the order

$Cl^- < Br^- < HS^-$; this resulted in an observed decrease in the curvature of the adsorbed aggregates (from spheres to short rods to cylinders) as the effective headgroup charge was reduced. The amount of counterion condensation was related to the polarizability of the ions and whether they are classified as "hard" or "soft".[28,31] A "soft" ion has a higher polarizability and will have a greater surface excess on the micelle because of its greater excess polarizability and hence greater dispersion forces. "Hard" ions, such as chloride, typically have a greater affinity for water and are more dissociated. While these arguments are appealing, and it seems reasonable that the vinyl benzoate ion used here is a "soft" ion, no account was taken of the attraction of a large organic counterion for the micelle core.[29] In the case of CTVB this would seem to be at least as important in the determination of its surface excess and hence the charge of the micelle.

Analysis of the force−distance data for CTVB on silica (Figure 4) indicates some important differences from that seen for the same molecules on mica (Figure 2). This is despite the apparent similarity of the imaged structures. The silica force data show an instability at approximately 12 nm separation. This is followed by a jump inward to a distance of 6.5 ± 0.5 nm where a nearly vertical section of data is then seen. Finally, there is a jump-to-contact from a distance of 4.2 ± 0.5 nm. These distances correspond well with previously reported data for CTA^+ aggregates with an acetate counterion. The diameter of a CTA^+ micelle is typically taken as twice the extended length of the CTA^+ molecule (4.5 nm). The jump-in distance corresponds well with this value suggesting that we have a layer of "full" cylinders in this case. The instability at 12 nm is due to interactions between the tip and surfactant layer prior to contact and push through. The associated uncertainties with separation distances in force data and push through distances prevent a fully quantitative comparison between the silica and mica data. However, since both sets of data were collected at the same electrolyte concentration, we may expect the interaggregate spacing to be constant (controlled by double layer repulsions). If this is so, the increased value of the mean separation inferred from the FFT data implies a significantly larger aggregate radius in the X−Y plane at the mica surface. Taken with the smaller push thorough distance, we infer a structure that has a more oblate appearance in cross section.

The effect of polymerization of the CTVB monomer on its bulk solution structure was previously investigated using small-angle neutron scattering (SANS).[19,20] The data indicated that after polymerization, aggregates with the same cross-sectional area were present.[19] However, the polymerization resulted in a solution of much lower viscosity. SANS and static light scattering[21] analysis of the resulting solutions show that the polymerized micelles are uncharged and have a shorter contour length (typically 100−200 nm) than their unpolymerized analogues. The aggregates are rigid rods in solution, probably due to the inherent stiffness of the poly(vinyl benzoate) polymer solubilized in the micelles. Finally, the lack of surface charge for the polymerized micelle indicates an extremely close association between the chain and the CTA^+ counterions.

An image of the structure for an adsorbed film of poly-CTVB at the mica−solution interface is shown in Figure 5. The corresponding force−distance behavior is given in Figure 6. Initial inspection of the image indicates the presence of a locally highly organized film of parallel cylinders. There also appears to be some large-scale debris
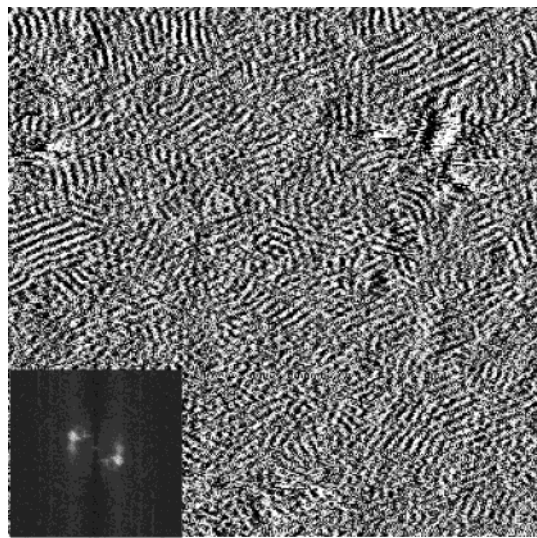

Figure 5. A 500-nm AFM deflection image of poly-CTVB at the mica−solution interface. The images were obtained in situ, at a polymer concentration of 0.8 g/L. The image indicates the presence of highly organized local regions of approximately 50 nm × 50 nm. The inset to this figure shows the Fourier transform of the data.
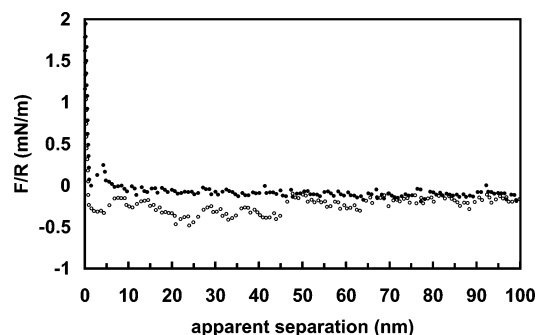

Figure 6. Force as a function of separation distance for the interaction between a silicon AFM tip and a mica surface in 0.8 g/L poly-CTVB. Data are shown for both the approach (filled) of the tip to the surface and its retraction (open). The multiple adhesive events seen during the retraction are characteristic of a polymeric adsorbate.

that is most likely present as a byproduct from the free-radical polymerization reaction. Such debris is known to have a detrimental effect on surface order causing dislocations in adsorbed films.[32] The high degree of order seen in the image is supported by the transform of the data; analysis of these data indicates a mean aggregate spacing of 8.3 ± 0.3 nm.

Comparison of these data with that shown in Figure 1 for the unpolymerized system highlights a number of important differences. Although in the bulk the cross sections of the unpolymerized micelles and polymerized micelles are the same, the center-to-center distance of the aggregates adsorbed on mica is smaller in the polymerized case. The cylinders in the polymerized case appear to be "straighter" but shorter. This is consistent with the bulk information obtained from SANS for the polymerized micellar system. The increased "straightness" must correlate with an increase in the intrinsic stiffness of the micelles after polymerization. Further evidence that we are imaging an adsorbed film of the polymerized micelles is found in the force−distance data for this system. First, there is little evidence of a long-range double layer

(31) Ninham, B. W.; Yaminsky, V. *Langmuir* **1997**, *13*, 2097−2108.

(32) Wanless, E. J.

interaction on the approach of the two surfaces. Again, this supports a central conclusion of the SANS analysis that the polymerized micelles have a net neutral charge. At a distance of approximately 6 nm a small almost vertical repulsion in the data set is observed. At a distance of 4.2 nm, an instability in the force data is seen and the tip jumps toward the surface, pushing through the adsorbed film. The push-through distance compares very well to that seen above for the unpolymerized sample on silica confirming the hypothesis that the cylindrical cross-section size is unaltered by the polymerization. The retraction data, collected as the surfaces are separated after contact, shows a number of adhesive events prior to complete separation at a distance of about 60 nm. Such multiple adhesion events are typically seen for the interaction between surfaces bearing an adsorbed polymer layer.[33] Each adhesive event is interpreted as being due to the detachment of a polymeric loop or tail from one surface. The final adhesive breakage is assumed to be due to the detachment of a single highly extended chain. The fact that we observe such multiple adhesive events reinforces our expectation that the observed micellar aggregates are polymeric in nature.

It should also be noted here that the poly-CTVB samples were consistently easier to image than the nonpolymerized analogues. This is despite the absence of a repulsive double layer interaction in both cases. The most likely cause of this observation is also as a result of the polymeric nature of the aggregates. In general, for surfactant systems it is known that the approach of the tip toward the surface in the presence of a repulsive potential will lead to some desorption of the monomeric surfactant molecules.[28] Further, when the tip pushes against the layer, the ease of penetration is thought to be due to lateral mobility of the molecules out of the confined region between the tip and surface. In the case of the polymeric aggregates, the aggregate itself has considerable structural integrity through the chemical bonds along the polymeric backbone. This will reduce the ease of diffusion from between the tip and surface. The large adhesion energy of a polymer at an interface will also decrease the tendency for the aggregate to move out of the gap. Hence, the adsorbed film is more resistant to the probe and the layer is easier to image.

For comparison, data were also collected at the silica–solution interface. A typical image of the adsorbed film that results is shown in Figure 7. Although less clear than on mica, the image indicates once again the presence of a close packed layer of adsorbed cylindrical micelles. Analysis of the image indicates that the mean interaggregate spacing in this case is 7.2 ± 0.3 nm. The force–distance data (not shown) are essentially the same as those seen on mica (Figure 6). The magnitude of the push through was the same, 4.2 ± 0.2 nm. Furthermore, there was no evidence of a long-range double layer interaction and the adhesion data also confirm that the adsorbed aggregates are polymeric in nature. On the basis of the force data, particularly the push-through distances, we believe that the underlying surface has little effect on the structure of the adsorbed aggregate and it essentially retains its spherical cross section. There is a small change in the mean aggregate spacing between the two surfaces although both surfaces appear to support a close packed film of the polymerized micelles.

In a second series of experiments, charge was introduced into the polymerized micelle system through the addition
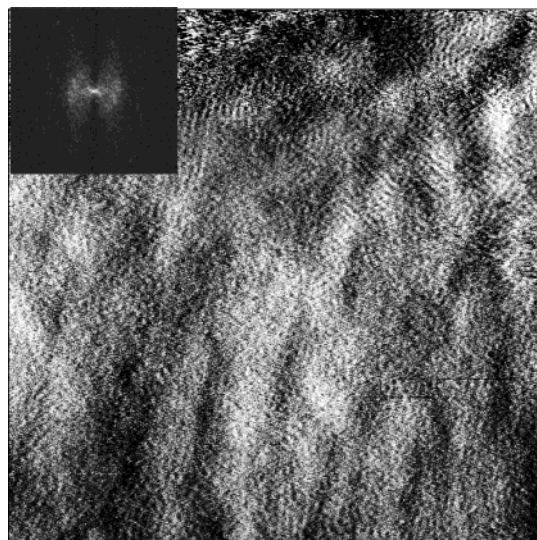
(33) Butt, H. J.; Kappl, M.; Mueller, H.; Raiteri, R.; Meyer, W.; Ruhe, J. *Langmuir* **1999**, *15*, 2559–2565.

Figure 7. A 500-nm AFM deflection image of poly-CTVB at the silica–solution interface. The images were obtained in situ, at a polymer concentration of 0.8 g/L. The inset to this figure shows the Fourier transform of the data.
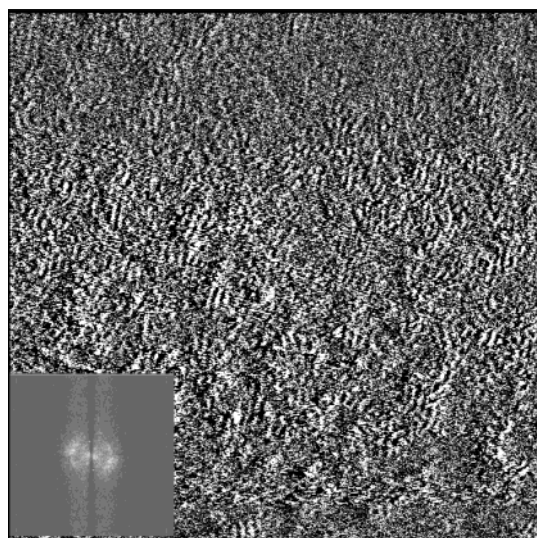

Figure 8. 500-nm AFM deflection image of adsorbed CTVB: NaT at the mica–solution interface. The images were obtained in situ, at a total surfactant concentration of 0.13 g/L using a soft-contact imaging protocol. The surface has a "lumpy" appearance with local regions where cylinders are clearly visible. The inset to this figure shows the Fourier transform of the data.

of a comonomer, sodium vinyltosylate (NaVT), into the CTVB system. During the polymerization of this system, the vinyl tosylate from both the CTVB and NaVT are polymerized into the polymer backbone; however the Na$^+$ ions can dissociate more readily than the CTA$^+$ ions resulting in aggregates with a net charge. Prior to discussion of the results for the polymerized system, it is again pertinent to present results for the adsorption of an unpolymerized analogue. As an analogue, we studied an adsorbed layer of a mixture of CTVB and sodium tosylate (NaT). While not an exact analogy for poly-CTVB:NaVT, the NaT was used due to availability and as a demonstration of the subtle effects of counterion in the adsorbed layers.

Figure 8 shows an image of the equilibrated adsorbed layer formed at the mica–solution interface by a 2:1 mixture (mol/mol) of CTVB (1.86 mM) and NaT (0.93 mM).

The image clearly indicates a surface that is covered in cylindrical aggregates. However, when compared to the corresponding image for pure CTVB (Figure 1), the surface has a "lumpy" appearance and there seems to be many more defects in the film. Ordered regions typically persist over only 20–40 nm^2 of the mica surface. A Fourier transform of the data is shown as an inset to Figure 8; this transform of the image shows considerably more angular structure than the peaks of other images. Multiple peaks are observed within the ring structure, indicating higher levels of structure in the surface. Analysis of the data indicates that there is a mean spacing of 8.3 ± 0.3 nm.

Adsorbed films that have a "lumpy" appearance have been reported previously for 1.8 mM CTAB solutions (2 × cmc) in the presence of a significant excess of 101 mM KBr.[24] In bulk, such a system is expected to form elongated wormlike micelles. At the mica–solution interface, the high concentration of electrolyte results in strong competition for the surface charged sites between the CTA$^+$ and K$^+$ ions. The resultant images showed cylindrical aggregates having significant defects and local ordered regions of 30–50 nm^2. The defects in the adsorbed layer were attributed to the disruption of CTA$^+$ adsorption caused by the presence of significant amounts of K$^+$ at the interface. It is interesting to discuss here whether a similar competitive adsorption process is occurring. In our case, the concentration of surfactant, CTVB, is 1.86 mM (~12 × cmc) while the concentration of the electrolyte, NaT, is 0.93 mM. This concentration of electrolyte is low and in the case of CTAB, for example, would be insufficient to compete effectively for surface binding sites. Further, the choice of cation here (Na$^+$) would also reduce the degree of surface binding when compared to the larger and less strongly hydrated K$^+$ ion. It was noted above that in the pure CTVB system the association between the ions is so strong that it prevents the CTA$^+$ ions competing effectively with the K$^+$ ions of the mica lattice for adsorption sites. It seems unlikely therefore that addition of the NaT, which can only result in more cation competition, would affect this situation and so we can rule out the surface as the cause of the increased disruption. Thus, the origin of the defects in the structure and the lumpy appearance is not due to competitive adsorption of ions at the interface.

We have already observed that micelles of CTVB carry only a limited charge which is presumably due to a combination of the bulky organic character of the counterion and its polarizability resulting in significant association between the ions at the micelle surface.[27–31] Examination of the chemical structure of the tosylate ion reveals its similarity to the vinylbenzoate ion. It seems likely therefore that a significant binding of these ions to the surface of the micelle aggregates will occur. This is confirmed when we examine typical force–distance data for the CTVB:NaT system at the mica–solution interface (Figure 9) where a significant long-range electrostatic component is seen. The charge seen in this case must originate in part from the incorporation of the NaT within the observed micellar structures. The charging of the micellar layer may then be used to explain the disruption of the adsorbed structure. Increased charge within a micellar aggregate is known to drive an increased curvature for those aggregates.[26] An increase in the effective repulsion within the cylindrical CTVB aggregates clearly results in an increased frequency of terminations for the cylindrical aggregates as would be expected if the average degree of curvature has been reduced. The force–distance data confirm the presence of aggregates. The push-through distance of 3.7 ± 0.2 nm is smaller than
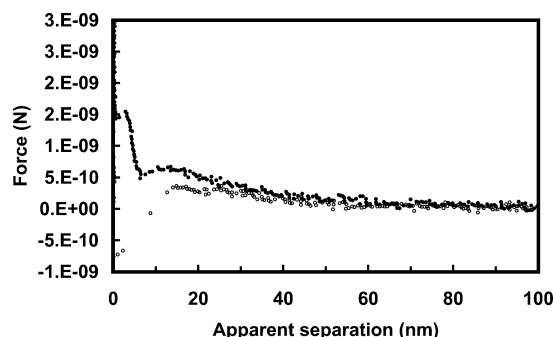

Figure 9. Force as a function of separation distance for the interaction between a silicon AFM tip and a mica surface in 0.13 g/L CTVB:NaT. Data are shown for both the approach (filled) of the tip to the surface and its retraction (open).
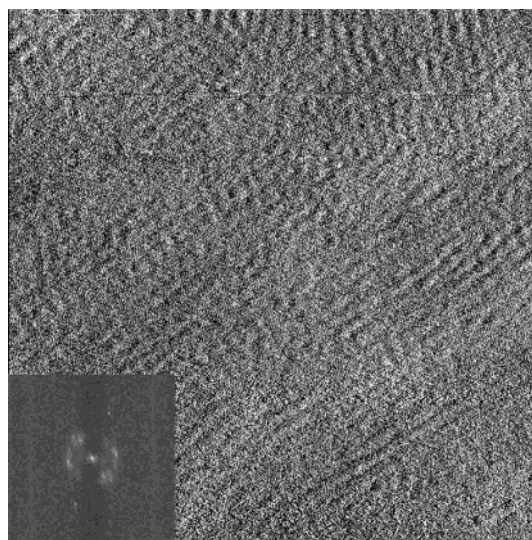

Figure 10. 250-nm AFM deflection image of adsorbed CTVB:NaT at the silica–solution interface. The images were obtained in situ, at a total surfactant concentration of 0.13 g/L using a soft-contact imaging protocol. The surface image indicates the presence of cylindrical aggregates. The inset to this figure shows the Fourier transform of the data.

that expected for a spherical CTA$^+$ aggregate and possibly indicates again a partial flattening of the adsorbed aggregates on mica. The retract data show a single pull-off confirming that the aggregates are molecular and not polymeric.

Examination of the same CTVB:NaT system at the silica–solution interface reinforces the view that the increased charge in the micelle causes a disruption of the adsorbed micelle structures. A representative image of the resultant surface aggregate structures seen at the silica–solution interface is given in Figure 10. The force–distance data were similar to that recorded on mica and are not given here. It should be noted however that the push-through distance seen was larger (4.3 ± 0.2 nm) and is consistent with spherical aggregate structures. Once again, the differences in the silica and mica data are consistent with the data seen for the CTVB system. Examination of the image indicates a surface covered in short rods and/or spheres caused by an increased number of defects and cylinder terminations. This is again consistent with an increase in the overall curvature caused by an increased charge. Analysis of the Fourier transform for these data indicates a mean aggregate spacing of 6.9 ± 0.2 nm. This is smaller than that seen for the mica surface and implies again that the aggregate shape on silica is more spherical than that on mica.
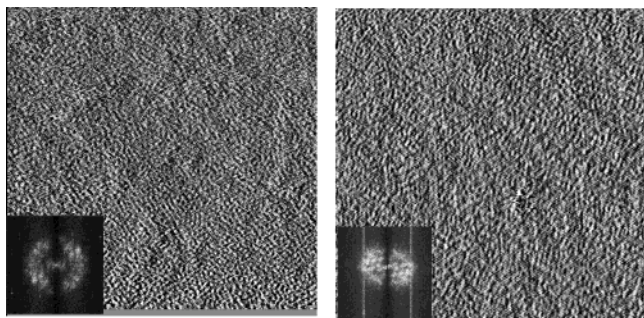
Figure 11. Two 500-nm AFM deflection images of poly-CTVB: NaVT at the mica−solution and silica−solution interfaces, respectively. The images were obtained in situ, at a polymer concentration of 1.0 g/L using a soft-contact imaging protocol. Both images indicate surfaces that are covered in spherical aggregates. The inset to this figure shows the Fourier transform of the data.
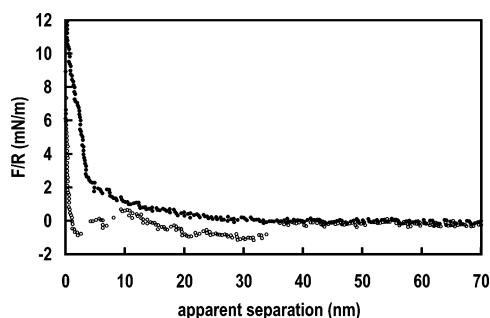

Figure 12. Force as a function of separation distance for the interaction between a silicon AFM tip and a mica surface in 1.0 g/L poly-CTVB:NaVT. Data are shown for both the approach (filled) of the tip to the surface and its retraction (open). The multiple adhesive events seen during the retraction are characteristic of a polymeric adsorbate.

The bulk structures of the CTVB:NaT and poly-CTVB: NaVT systems have not been quantified as extensively as CTVB and poly-CTVB. Solutions of CTVB with added NaT or NaVT are still viscoelastic and clear, indicative of wormlike micelles. The polymerization of CTVB:NaVT results in a low viscosity solution, indicating that the polymerization decreased the length of the micellar aggregates; this is similar to the behavior observed in polymerization of CTVB. SANS of the poly-CTVB:NaVT indicates that the micellar cross section is 1.9 nm, but the length and flexibility of the aggregates are unclear.[34] SANS indicates electrostatic interactions, even at low concentrations, but these interactions can be screened with the addition of sodium chloride.

Images of the structure of an adsorbed film of poly-CTVB:NaVT at both the mica−solution and the silica−solution interfaces are shown in Figure 11. A representative force−distance curve is given in Figure 12. Initial inspection of the images shows once again that the surface structure is consistent regardless of the underlying surface. Interestingly, in this case the surfaces appear to be covered by a system of close-packed spherical aggregates. The presence of polymerized micellar aggregates is confirmed from the retraction data of the force−distance plot. Once again, multiple adhesive events are observed. This contrasts with the unpolymerized case (Figure 9) where the breaking of the surface−surface adhesion always results in a clean separation of the surfaces. Thus, we can confirm directly that the observed aggregate
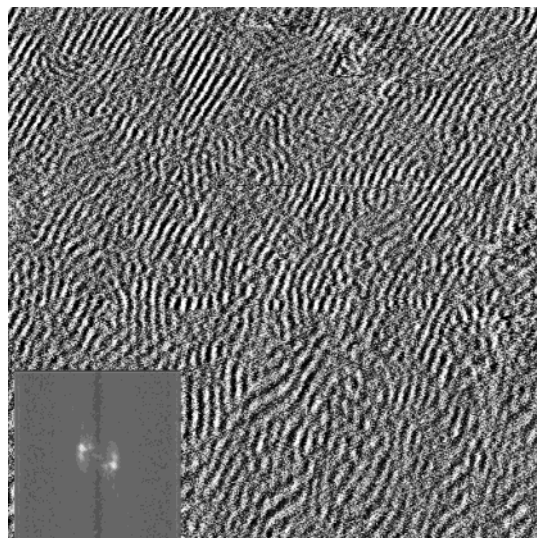

Figure 13. A 300-nm AFM deflection image of poly-CTVB at the mica−solution interface after soaking in pure water for 16 h. No desorption is seen when compared to the original images collected with polymer in the bulk.

structures originate from the polymerized micellar aggregates. In this case, however, the resultant aggregate after polymerization appears to have a "string of pearls" type structure.[35] Once again, the incorporation of an increased charge into the aggregate structure has resulted in an increase in the observed local curvature. Significantly, the charged comonomer must be closely associated with the CTVB aggregates giving them an "effective" charge. Note that there is conclusive proof that the poly-CTVB system is effectively uncharged. Thus the large organic anion of the NaVT is successfully incorporated into the polymeric counterion of the CTA$^+$ and is closely associated with the micellar aggregates. The charged nature of the aggregates is again confirmed from the force−distance data that indicate the presence of a long-range electrostatic repulsion as the surfaces are brought together.

The Fourier transform data for the poly-CTVB:NaVT systems are also given as insets to Figure 11. These data indicate that there is significant order in this system although not a perfect hexagonal close-packed layer. This is perhaps not surprising since there may well be a different spacing between two aggregates attached to the same polymer chain and two aggregates of a different polymer chain. Furthermore, there is no indication of whether the chains can cross one another in this surface structure or whether they are constrained to lie parallel to one another. The mean aggregate spacing is 8.4 ± 0.2 nm on mica and 8.1 ± 0.2 nm on silica.

Whatever the detailed nature of the arrangement of the polymer chains at the interface, it is clear that the addition of a small quantity of a charged comonomer into the system has resulted in a significant change in the polymeric aggregate structure. Once again, however, we have produced a system that is largely insensitive to the underlying surface structure.

An original motivation for the use of such polymeric surfactant aggregates as surface adsorbed films was the possibility that they would be resilient to solvent exchange and washing as well as drying and rehydration. In the bulk, it is already known that the polymeric aggregates can be evaporated to dryness and successfully rehydrated

(34) Kline, S. R. Unpublished results.

(35) Goddard, E. D. *Colloids Surf.* **1986**, *19*, 255−300.

with no loss in structure. In Figure 13, an image of an adsorbed film of poly-CTVB at the mica−water interface is presented. This image was obtained after an equilibrium adsorbed layer (Figure 5) was washed with an approximately 30-fold excess of water and subsequent soaking for 24 h. Direct comparison of this image with that given in Figure 5 indicates clearly that the washing phase has removed the surface debris. However, the adsorbed film is clearly not degraded despite prolonged exposure to pure water. Application of the same washing and soaking cycle to the poly-CTVB:NaVT films also resulted in no degradation of the adsorbed layers. In contrast, all of the nonpolymerized systems were completely removed after washing with pure water. The polymeric nature of the aggregate structures is sufficient therefore to prevent their desorption into pure solvent. This result is highly significant since it opens the possibility for multistep processing using such layers. Furthermore, the layers are expected to have all the advantages of the local character of an adsorbed surfactant film, particular in the nanostructural aspects of that layer.

Conclusions

Polymeric micellar aggregates adsorb at the solid−liquid interface forming a self-organized monolayer film. These films have many similar features to the films formed by simple surfactants; they are true nanostructures and they have a local but controlled heterogeneous microstructure. However, the polymerized systems form two-dimensional adsorbed films that are effectively permanently adsorbed. Rinsing of the films was not seen to result in any desorption. This ability to rinse the films facilitates further processing of these surfaces, significantly increasing their utility as surface templates or as drug delivery systems.

LA0358062